Quantifying lateral bedrock erosion caused during a hyperconcentrated flow in a narrow alpine limestone gorge

Verena Stammberger[1*], and *Michael* Krautblatter[1]

[1]Technical University of Munich, Chair of Landslide Research, 80333 Munich, Germany

Abstract. Here, we show results of an unprecedented LiDAR dataset quantitatively determining the lateral bedrock erosion of a narrow limestone gorge during an extreme hyperconcentrated flow. The comparison of two point clouds prior and post to the June 15th hyperconcentrated flow event provide information about the massive breakout of particles and abrasion of the channel walls. With a multiscale model to model cloud comparison analysis, we can show that particles from 0.0001 m^3 and 3.5 m^3 were eroded from the subvertical limestone gorge walls. A total of 20.9 m^3 of massive bedrock was eroded in the observable part of the channel with 90 % of the particles being smaller than 0.15 m^3. We delimited two main erosion processes during the hyperconcentrated flow event: shearing of particles that reach into the flow and particles with predefined failure surfaces, and abrasion along the whole channel, detectable by LiDAR if the changes are > 3 cm. This study provides quantitative evidence for massive rock erosion processes in alpine gorges that could also control rock gorge formation and evolution over Holocene/Lateglacial time scales.

1 Introduction

An increase of annual heavy precipitation events [1] as well as climate-related extremes such as floods [2] is likely in near-future developments in climate change. This is directly linked to the occurrence of debris flows and hyperconcentrated flows of which both can pose severe risk to human life [3]. Due to the massive forces that can act during hyperconcentrated flows, they have high potential of causing geomorphic changes along the flow path [4]. Several studies showed the erosion and entrainment of loose sediment [5-8] which can cause a massive increase of the mobilised flow volume. Also a vast amount of studies discusses fluvial channel incision by a saltating bed causing abrasion, plucking or cavitation [9-14]. But only very sparse data is available describing the erosive power of debris flows on bedrock channels either by field observations [15,16] or laboratory experiments [17]. Here, we present unprecedented data that quantitatively and qualitatively describes the geomorphic changes due to lateral erosion in a narrow limestone gorge caused by a hyperconcentrated flow event.

2 Study area and flow event

On the 13th of June 2020, a local extreme precipitation event of 50 to 60 mm/h (DWD, Radar measurements) caused a hyperconcentrated flow event in the Höllentalklamm, a gorge situated in the Wetterstein mountains, Germany (see Fig. 1). The channel lies between 1032 and 1062 m a.s.l. and drains a catchment of 10 km^2 with the Zugspitze (2968 m a.s.l.) marking the highest point. Due to the steep slopes of the catchment (inclination of ø 110%) a rapid accumulation of the surface runoff caused a massive mobilization of secondary sediment storages which were then transported to the upper entrance of the gorge. Throughout the narrow ravine, massive dispersive forces reshaped the channel walls by particle erosion, shearing, abrasion and shifting of boulders up to 20 m^3. The gorge as well as the above catchment consist of Mid Wetterstein limestone [18].

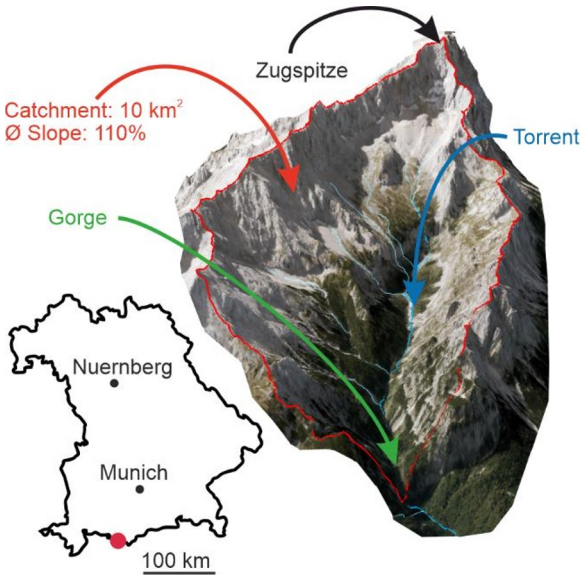

Fig. 1. Location of the study site in southern Bavaria (red dot) and 3D-view of the catchment and position of the gorge. Orthophoto: www.geodaten.bayern.de.

* Corresponding author: verena.stammberger@tum.de

3 Methods

We conducted a terrestrial LiDAR campaign using a RIEGL VZ-400 laser scanner to record the changes caused by the hyperconcentrated flow event. The reference data was acquired on the 28th of May, initially for a biannual rockfall monitoring of the gorge. The second scanning campaign was shortly after the event (19th and 25th of June). In total, we recorded 84 single scans positioned along the approximately 900 m long gorge. The angular step was set between 0.04 and 0.06° with an angle measurement resolution below 0.0005°. Due to the complex environment with overhanging walls and a windy channel, some data gaps result from occlusion, thus are unavoidable. The point cloud alignment was applied in RiSCAN Pro 2.9 with an iterative closest point (ICP) algorithm [19-21]. By minimizing the difference of corresponding planes in two subsequent scans, a co-registration with standard deviation below 1 cm was achieved. We reduced the point densities to 2.5 cm in XYZ direction to prevent any bias due to a heterogeneity of the clouds. To georeference the resulting point clouds of the whole gorge, we used an airborne lidar dataset recorded in 2006.

We applied the Multiscale Model to Model Cloud Comparison (M3C2) to estimate the geomorphic changes [22] in this morphologically complex gorge. This algorithm allows to calculate changes perpendicular to the rock face and eliminate high artificial values close to data gaps. We analysed the sides of the bedrock channel to quantify the lateral erosion. Due to the water discharge in the channel, we were not able to calculate the vertical incision at the bed. The detected changes are classified in either *statistically significant* (change > level of detection) or *not statistically significant* and rejected. Thereafter, we validated all statistically significant changes manually to eliminate further errors. We then calculated the area and volume by triangulating the isolated point clouds of the single particles/coherent erosion areas (hereafter both referred to as 'particles'). By projecting the corresponding clouds onto a surface perpendicular to the rock face and calculating the difference. For further analysis of the erosion volumes along the channel, we divided the pointclouds of the gorge in 10 m-sections and summed up the eroded particle volumes for each section.

Simultaneously to the LiDAR measurements, we recorded the state of the gorge after the hyperconcentrated flow event with a 360° camera. Some earlier photographs of the gorge during previous rockfall monitoring campaigns supported the comparison. Visual colour changes of the bedrock surface were identified to determine a minimum flow height h_{HCF} throughout the entire flow path of the channel (see Fig. 2). Using the pointclouds we determindes the altitude of the channel bed elevation (dashed lines in Fig. 2).

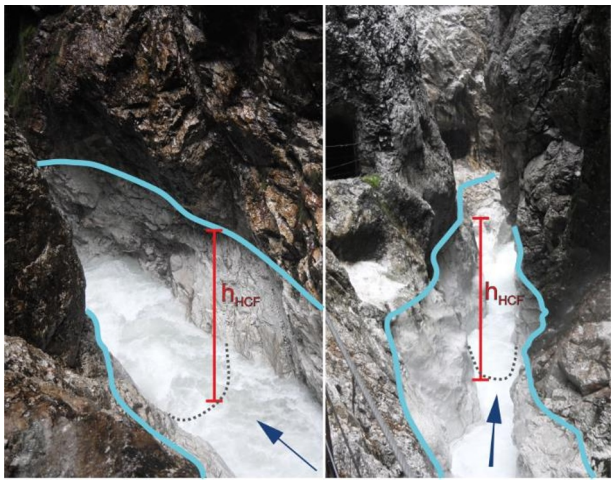

Fig. 2. Visual determination of the flow height of the hyperconcentrated flow throughout the gorge. Affected bedrock areas show a brighter colour due to abrasion.

4 Results

We were able to determine the minimum flow height of the hyperconcentrated flow throughout the whole channel of the mountain gorge by analysing the photographs pre- and post-event at more than 50 positions. The mean flow height along the 900 m long gorge revealed 2.8 m and a calculated maximum flow height of 12.3 m. However, these values are influenced by a steep drop of the channel creating a waterfall. For the remaining part of the channel, the maximum flow height is 7.2 m and the minimum height is 0.5 m.

Using the M3C2 change detection analysis we detected 232 particles that were eroded during the June 2020 hyperconcentrated flow event. The smallest detected particles volume equals 0.0001 m^3, the largest is a block of 3.30 m^3. 90 % of the changes are below 0.15 m^3 (see Fig. 3) but account for only 25 % of the eroded volume. A total volume of around 20.6 m^3 of limestone bedrock was eroded laterally from the channel sides. The corresponding eroded area is 137 m^2. This yields a mean erosion depth of 15 cm for the areas indicating significant change.

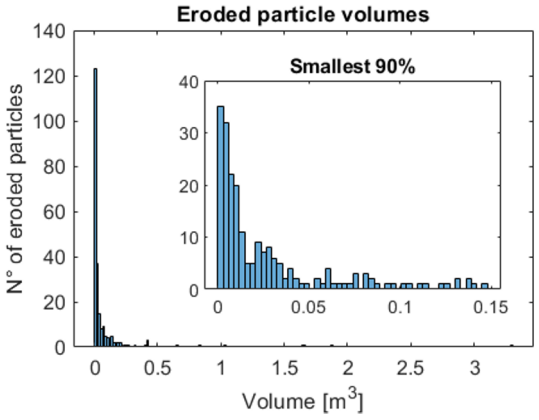

Fig. 3. Histogram of the detected eroded bedrock particle volumes along the channel sides (outer figure) and histogram of the smallest 90 % of detected eroded particles (inner figure)

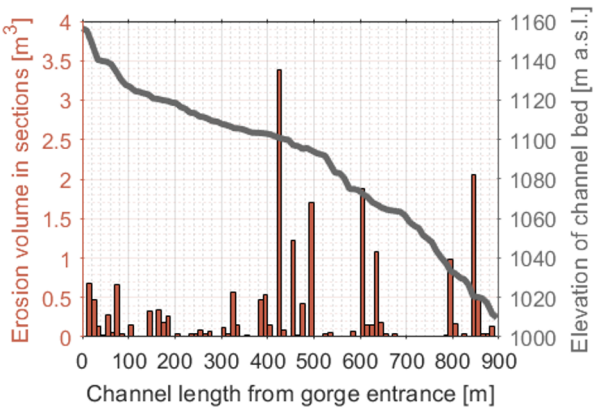

Fig. 4. Detected erosion volumes in the defined 10 m-sections (left axis) and gorge channel bed elevation (right axis)

Dividing the gorge in 10 m-parts along the channel axis resulted in a total of 89 subparallel sections. The total erosion volume of each section is the sum of the eroded particle volumes lying in between the dividing profiles. In 27 of the 89 sections (30 %), we did not detect any erosion with the M3C2 analysis. The mean erosion volume per section in which erosion was detected is 0.33 m^3. In Fig. 4 the erosion volumes per section are plotted at the position along the channel bed and the elevation of the bed.

5 Discussion

The field investigations and photographic records of the whole gorge clearly showed that the hyperconcentrated flow event caused extreme changes to the limestone gorge. Formerly weathered bedrock surfaces on the sides of the channel show a distinct colour change due to a constant abrasion of the uppermost layer. As we identified this border of abraded and weathered rock surface, we were able to define the minimum flow height of the hyperconcentrated flow along the whole channel. This height is not necessarily the absolute flow height of the event, a layer of water flow with less suspended sediment above the heavily charged bottom layer is possible. This hypothesis is further supported by some sediment deposits above the defined minimum flow height.

The maximum calculated flow height is influenced by a drop within in the channel creating a waterfall. Nevertheless, we detected erosion caused by abrasion in some distance to the drop. This reveals the high discharge during the event that led to a hose-effect and an increased casting distance. As expected, the flow height in the remaining channel is heavily dependent on the width of the cross sections.

The M3C2 analysis showed a total lateral bedrock erosion volume of 20.6 m^3 from 232 particles throughout the gorge. This only accounts for the erosion from the rock walls and does not quantify erosion from the channel bed nor any entrainment of loose sediment. The detected changes can be explained with two different mechanisms that are manually distinguished by their pre- and post-event geometry. i) we assume that particles with a geometry that is prone to shearing during the flow (nose-like) are broken out of the channel walls. Likely the same happens with particles with predefined loose joints. The driving (shearing) forces succeed the holding forces of the rock or rock-bridges. This process might be driven by plucking but even more so by the increased yield strength of the flow that forces the breakout of particles in the rockwalls. ii) massive abrasion of the bedrock by the suspended particles within the flow describes the second mechanism. Based on photographs we visually recorded the results of the abrasion process along the channel. In places with massive abrasion of more than 3 cm depth we were able to detect it in the change detection analysis. These changes are characterized by a smooth erosion surface rather than a spikey one. Around the edges, the detected changes between the pointclouds are usually the smallest and in the centre it shows the maximum erosion depth.

Subdividing the channel in 10 m sections can give first information about the spatial occurrence of the eroded volumes. The first 350 m are characterized by smaller changes with less variation and only a few sections without any detected change. Most of the changes are located in the middle part of the gorge (Fig. 4). The middle part between 350 and 700 m is the part with the most eroded volume and great variation of the erosion volume per section. In the third section there is a large fraction with no erosion and again very high changes.

6 Conclusions

We were able to record the geomorphic change and massive rockwall erosion in an alpine limestone gorge caused by a hyperconcentrated flow event in June 2020. An unprecedented LiDAR dataset quantitatively shows the lateral bedrock erosion along the channel walls. Additionally, we were able to detect visual changes to the bedrock channel walls and recorded them with photographs. In conclusion, we delimited two mechanisms of particle or bedrock erosion during a hyperconcentrated flow event:
i) *Abrasion* process: along the whole channel, detected visually for changes < 3 cm erosion depth and detected with the LiDAR data for changes > 3 cm
ii) *Shearing* process: shearing force acts on areas with a geometry that reaches into the flow (nose-like) and on particles with predefined failure surfaces.

This study shows and provides quantitative insights to rapid erosion processes in alpine gorges. Extreme events like the observed hyperconcentrated flow or debris flows might account for a larger proportion of bedrock erosion in channels than previously thought. Over longer timescales, they could even act to control rock gorge formation and evolution.

References

1. IPCC, *Climate Change 2013. The Physical Science Basis*, Cambridge University Press (2013)

2. IPCC, *Climate Change 2014. Impacts, Adaptation, and Vulnerability. Summaries, Frequently Asked Questions, and Cross-Chapter Boxes*, Cambridge University Press (2014)
3. C.A. Dowling, P.M. Santi, Nat. Hazards **71**(1), 203-227 (2014)
4. T.C. Pierson, *Distinguishing between debris flows and floods from field evidence in small watersheds*, USGS Fact Sheet, 2004-3142, Vancouver (2005)
5. C. Berger, B.W. McArdell, F. Schlunegger, J. Geophys. Res., **116**(F1) (2011)
6. S.W. McCoy, J.W. Kean, J.A. Coe, G.E. Tucker, D.M. Staley, T.A. Wasklewicz, J. Geophys. Res., **117** (F3), (2012)
7. M. Bremer, O. Sass, Geomorphology, **138** (1), 49–60 (2012)
8. A: Dietrich, M. Krautblatter, Earth Surf. Process. Landforms **44** (6), 1346–1361 (2019)
9. M.A. Seidl, W.E. Dietrich, *The Problem of Channel Erosion into Bedrock*, Functional geomorphology, Catena Supplement, **23**, 101–124 (1992)
10. K.X. Whipple, G.S. Hancock, R.S. Anderson, Geol. Soc. Am. Bull., **112** (3), 490–503 (2000)
11. L.S. Sklar, W.E. Dietrich, Water Resour. Res. **40** (6), (2004)
12. M. Schaller, N. Hovius, S.D. Willett, S. Ivy-Ochs, H.A. Synal, M.C. Chen, Earth Surf. Process. Landforms, **30** (8), 955–971 (2005)
13. L. Anton, A.E. Mather, M. Stokes, A. Muñoz-Martin, G. Vicente, *Exceptional river gorge formation from unexceptional floods*, Nat. Commun. **6** (2015)
14. A.L. Marcotte, C.M. Neudorf, A.L. Langston, Earth Surf. Process. Landforms **46** (11), 2248–2263 (2021)
15. J. Stock, W.E. Dietrich, Water Resour. Res. **39** (4), (2003)
16. E.R.C. Baynes, M. Attal, S. Niedermann, L.A. Kirstein, A.J. Dugmore, M. Naylor, *Erosion during extreme flood events dominates Holocene canyon evolution in northeast Iceland*, in Proc. Natl. Acad Sci. U.S.A., **112** (8), 2355–2360 (2015)
17. N.J. Finnegan, L.S. Sklar, T.K. Fuller, J. Geophys. Res. **112** (F3) (2007)
18. H. Miller, *Zur Geologie des westlichen Wetterstein- und Mieminger Gebirges (Tirol). Strukturzusammenhänge am Ostrand des Ehrwalder Beckens*. LMU Munich (1962)
19. P.J. Besl, N.D. McKay, *A Method for Registration of 3-D Shapes*, IEEE Trans. Pattern Anal. Mach. Intell. **14** (2), 239–256 (1992)
20. Y. Chen, G. Medioni, *Object modeling by registration of multiple range images*, Image Vis. Comput. **10**, 145–155 (1992)
21. Z. Zhang, Int. J. Comput.Vis. **13** (2), 119–152, (1994)
22. D. Lague, N. Brodu, J. Leroux, *Accurate 3D comparison of complex topography with terrestrial laser scanner: Application to the Rangitikei canyon (N-Z)*, ISPRS J. Photogramm. Remote Sens **82**, 10–26 (2013)